Pergamon

Geochimica et Cosmochimica Acta, Vol. 68, No. 10, pp. 2245–2258, 2004

0016-7037/04 $30.00 + .00

doi:10.1016/j.gca.2003.11.009

Diagenesis and the reconstruction of paleoenvironments: A method to restore original $\delta^{18}O$ values of carbonate and phosphate from fossil tooth enamel

ANTOINE ZAZZO,[1,2,*] CHRISTOPHE LÉCUYER,[3,4] SIMON M. F. SHEPPARD,[5] PATRICIA GRANDJEAN,[3] and ANDRÉ MARIOTTI[4,6]

[1]Department of Geological Sciences, University of Saskatchewan, 114 Science Place, Saskatoon, SK S7N 5E2, Canada
[2]Dynamique de l'Evolution humaine, CNRS UPR 2147, 44 rue de l'Amiral Mouchez, 75014 Paris, France
[3]Laboratoire "Paléoenvironnements and Paléobiosphère" CNRS UMR 5125, Batiment Géode, Campus de la Doua, Université Claude Bernard Lyon, 69622 Villeurbanne, France
[4]Institut Universitaire de France, 103 boulevard Saint-Michel, 75005 Paris, France
[5]Laboratoire de Sciences de la Terre, CNRS UMR 5570, Ecole Normale Supérieure de Lyon, 46 allée d'Italie, 69364 Lyon Cedex 07, France
[6]Laboratoire de Biogéochimie des Milieux Continentaux, UMR 7618 INRA-CNRS-IRD, IFR EGER 106, Université Pierre et Marie Curie, 78850 Thivernal-Grignon, France

(*Received July* 15, 2003; *accepted in revised form November* 17, 2003)

Abstract—Intra-tooth $\delta^{18}O$ variations within the carbonate ($\delta^{18}Oc$) and phosphate ($\delta^{18}Op$) components of tooth apatite were measured for Miocene and Pliocene hypsodont mammals from Afghanistan, Greece and Chad in order to evaluate the resistance of enamel to diagenetic alteration. Application of water-apatite interaction models suggest that the different kinetic behaviours of the phosphate-water and carbonate-water systems can be used to detect subtle oxygen isotope disequilibria in fossil enamel when intra-individual variations are considered. Selective alteration of the oxygen isotope composition from the carbonate component of Afghan and Greek enamels suggests inorganic isotopic exchange processes. Microbially-induced isotopic exchange for phosphate is demonstrated for the first time in enamel samples from Chad, in association with extensive recrystallization. In Chad, $\delta^{18}Op$ values were derived from partial isotopic exchange with fossil groundwater during early diagenesis. Mass balance calculations using average carbonate content in enamel as a proxy for recrystallization, and the lowest $\delta^{18}Op$ value of dentine as a proxy for the isotopic composition of the diagenetic fluid, indicate that diagenesis can alter $\delta^{18}Op$ by as much as 3‰ in some enamel samples. This diagenetic alteration is also responsible for a decrease in intra-individual variations of up to 1‰ in affected specimens. The effects of diagenesis on $\delta^{18}Op$ values of fossil enamel are not systematic, however, and can only be estimated if sequential $\delta^{18}Op$ and $\delta^{18}Oc$ analyses are performed on fossil enamel and dentine. Reconstruction of large temporal- or spatial-scale paleoclimates based on $\delta^{18}Op$ analyses from mammalian teeth cannot be considered valid if enamel has been affected by bacterial activity or if the data cannot be corrected for diagenetic effects. *Copyright © 2004 Elsevier Ltd*

1. INTRODUCTION

Two interesting properties of biogenic apatites led researchers to investigate the use of intratooth $\delta^{18}O$ variations in modern tooth enamel as an indicator of both seasonality and short-term climate change. Firstly, oxygen isotope compositions of carbonate ($\delta^{18}Oc$) and phosphate ($\delta^{18}Op$) bioapatites are closely related to that of ingested water in large mammals (Longinelli, 1984; Luz et al., 1984; Bryant and Froelich, 1995; Kohn, 1996). Secondly, in hypsodont mammals, enamel mineralization proceeds from the apex (upper part) to the cervix (lower part) of the crown as teeth emerge and tooth enamel is not remodeled once formed. As a result, successive growth increments of enamel record changes in the isotopic composition of water ingested by mammals during tooth mineralization (Fricke and O'Neil, 1996; Kohn et al., 1998).

Fossil mammalian hypsodont enamel is widely considered the material of choice for paleoclimatic reconstructions using stable oxygen isotope compositions of fossil bioapatite. Unlike bone, cement and dentine, enamel is considered to be more resistant to diagenetic alteration because it has a lower organic matter content and a higher degree of crystallinity (Trautz, 1967; LeGeros and LeGeros, 1984; Posner, 1987; Newesely, 1989; Ayliffe et al., 1994). Since the oxygen in P-O bonds is very resistant to inorganic isotope exchange with aqueous fluids at surface temperatures (e.g., Bunton et al., 1961; Blake et al., 1997; Lécuyer et al., 1999), $\delta^{18}Op$ values in fossil enamel are often considered pristine.

The effects of early diagenesis on the isotopic compositions of fossil enamel are not yet fully understood, especially in the presence of soil micro-organisms. Indeed, Zazzo et al. (2004) demonstrated experimentally that enamel crystallites could experience oxygen isotope exchange with soil water in the presence of bacteria and fungi. Moreover, the same authors showed that the pretreatment protocol currently used to remove exogenous carbonates (Lee-Thorp and van der Merwe, 1987; Koch et al., 1997) does not eliminate diagenetic signals.

To resolve the mechanism and impact of diagenetic alteration on the oxygen isotope composition of fossil enamel, we have to establish whether the diagenetic process is controlled inorganically or microbially. If inorganic reactions predominate during diagenesis, $\delta^{18}Oc$ values are expected to be more affected than $\delta^{18}Op$ values. If micro-organisms are involved during alteration processes, however, oxygen isotope exchange may occur between reacting aqueous fluids and oxygen in both phosphate and carbonate apatite. To date, the only criteria available for identifying post mortem isotopic exchange be-

* Author to whom correspondence should be addressed (antoine.zazzo@usask.ca).

tween bioapatite and its burial environment are (1) comparison of enamel $\delta^{18}O$ values with those of associated bone, cement, or dentine (Ayliffe et al., 1994; Sharp et al., 2000) or (2) comparison of coexisting $\delta^{18}Oc$ and $\delta^{18}Op$ values from the same sample (Iacumin et al., 1996; Fricke et al., 1998; Shahack-Gross et al., 1999). Neither approach yields information about the alteration process. Enamel-dentine comparisons only show if enamel is less altered than dentine, but do not prove that enamel is fully preserved, and plotting $\delta^{18}Oc$-$\delta^{18}Op$ pairs of bulk enamel or dentine samples against an equilibrium line detects isotopic disequilibria in the carbonate-phosphate system, but cannot unambiguously determine which phase has been altered. Additionally, neither approach offers a method to correct for diagenetic effects.

This study represents the first attempt to describe and model the effects of diagenesis on the oxygen isotope composition of fossil enamel. We propose a set of mass balance equations to quantify oxygen isotope offsets resulting from diagenetic alteration in carbonate and phosphate apatite. These equations may be applied successfully when combined with intratooth sampling and $\delta^{18}O$ analyses of hypsodont teeth. Our method reveals that the mechanism (microbially-mediated vs. inorganic) and intensity of isotopic alteration of carbonate and phosphate in apatite is highly variable as illustrated by Miocene and Pliocene samples from Afghanistan, Greece and Chad. Finally, we discuss how diagenetically derived modifications of isotopic compositions may impact the validity of paleoenvironmental and paleobiological reconstructions.

2. MATERIAL AND METHODS

2.1. Modern Material

Seven enamel samples of modern wild African hippopotamuses (*Hippopotamus amphibius*) were obtained from the European Museums of Tervuren (Belgium), Geneva (Switzerland) and Berlin (Germany). They were used to build an internal $\delta^{18}Oc$ vs. $\delta^{18}Op$ reference equation for modern apatite. For each sample, 100 to 150 mg of enamel were crushed in a mortar and pestle before homogeneization.

2.2. Fossil Material

Fossil teeth from Chad, Greece and Afghanistan were selected for this study. Fossil material from central Chad consists of four teeth from fossil equids (*Hipparion* sp.), which were found in three Pliocene levels called Kossom Bougoudi, Kollé and Koro Toro (Brunet et al., 1995, 1998; Brunet and MPFT, 2000). They are ~5.0 to 5.5, 5.0, and 3 to 3.5 Ma old, respectively, and spaced ~20 km apart. The youngest one (Koro Toro) yielded the first hominid remains west of the Rift Valley (Brunet et al., 1995). The region (Djurab Erg) is now a desert, but paleontological and isotopic evidence indicate that it was intermediate between mosaic forest-savannah environment (Brunet et al., 1997, 1998; Brunet and MPFT, 2000) and open savannah (Zazzo et al., 2000; Geraads et al., 2001) during the Pliocene. Fossils from Chad are dark in color, and are generally found at the surface or in subsurface sandstone deposits, sometimes partly covered with a Fe or Mn oxidized crust. Fossil material from Afghanistan consists of three bovid third molars (*Tragoportax* sp.), which were collected at the Upper Miocene locality of Molayan. The molars are yellowish and were removed from well-preserved mandibles that were highly concentrated in sandy-clayey deposits of fluvial origin (Sen, 1998, 2001). Data obtained from these Afghan bovid teeth were published in Zazzo et al. (2002). Another *Tragoportax* sp. third molar was also selected at the Upper Miocene locality of Ravin des Zouaves in Greece.

A sequence of 7 to 14 enamel samples for each tooth was drilled from the top to the bottom of the crown, following the growth axis of the tooth, with each sample spanning the entire enamel thickness. One to three samples of dentine were also selected in the upper, median and lower parts of each tooth. Because enamel and dentine mineralizations proceed from the apex to the cervix of the crown, down-tooth sequential sampling and isotope analyses of hypsodont teeth provide a record of environmental changes that occurred during tooth growth. This sampling methodology is frequently used for enamel to reconstruct past short-term seasonal changes in diet or climate (Fricke et al., 1998; Gadbury et al., 2000; Balasse et al., 2002). However, recent studies demonstrated that this sampling protocol is not adapted to the geometry of mineralization and is responsible for time averaging biases that underestimates the amplitude and timing of seasonal variations recorded within a tooth (Fisher and Fox, 1998; Balasse 2002; Passey and Cerling 2002). Since the goal of this study was not to restore faithfully the environmental variations, but rather to quantify the *postmortem* modifications of the original isotopic record, we followed the usual sampling protocol.

2.3. Analytical Procedures

Carbonate apatite powders were treated with a 2 to 3% sodium hypochlorite solution for 4 h to remove organic matter then rinsed three times with distilled water. Each sample was then split for carbonate and phosphate oxygen isotope analyses. before oxygen isotope analysis of the carbonate phase, samples were treated with a 1 mol/L acetic acid-acetate buffer for 24 h to remove exogenous carbonates (Bocherens et al., 1996), rinsed eight times with distilled water, centrifuged, and dried at 50°C overnight. About 10 mg of each enamel or dentine powder was then reacted with ~1 mL of anhydrous phosphoric acid for 5 h at 50°C under vacuum to extract CO_2 gas. Oxygen isotope ratios of CO_2 were measured on a Sira 9 mass spectrometer at the Laboratoire de Biogeochimie Isotopique (UPMC, Paris VI) with an analytical precision of ±0.2‰, determined from replications on a bioapatite internal standard. The carbonate content of each sample was determined by coulometry during acid digestion with an analytical precision of ±0.1 wt.%. About 30 mg of enamel were necessary to isolate biogenic phosphate as Ag_3PO_4 crystals following the procedure of Crowson et al. (1991) modified by Lécuyer et al. (1993). Measurements of $^{18}O/^{16}O$ ratios from Ag_3PO_4 were performed with a VG Prism mass spectrometer at the Ecole Normale Supérieure of Lyon, and with a DeltaE mass spectrometer at the Laboratoire Paléoenvironnements and Paléobiosphère (University of Lyon 1), using the method of Lécuyer et al. (1998) modified after O'Neil et al. (1994). Isotopic measurements were normalized to the international standards NBS-18 and NBS-19. Because the oxygen yield using the graphite method is only 25%, all data obtained with this method have been corrected from a constant offset of +0.5‰ that was observed during the intercalibration of both methods (see Lécuyer et al., 1998). We wish to emphasize that unlike the O'Neil et al. (1994) "sensu stricto" method, the Lécuyer et al. (1998) method does not require to apply a scaling factor to the data. Samples of NBS 120c (Florida phosphate standard) were analyzed repeatedly and gave an average $\delta^{18}O$ value of 21.7 ± 0.16‰. Results are expressed in "δ" per mil units (‰) relatively to SMOW, where $\delta = ([R_{sample}/R_{standard}]-1) \times 1000$, and R is the high-to-low mass isotope ratio.

3. RESULTS

The $\delta^{18}Oc$ and $\delta^{18}Op$ values of modern hippopotamuses show a good linear relationship (Fig. 1, Table 1). We used reduced major axis rather than least square regressions because this treatment is more appropriate when there are comparable errors in x and y. Regressions were computed for modern hippopotamuses (Eqn. 1), and previously published results (Eqn. 2, Bryant et al., 1996; Iacumin et al., 1996):

$$\delta^{18}Op = 0.974 \cdot \delta^{18}Oc\ (\pm 0.044) - 9.117\ (\pm 1.346)\ (n=7) \quad (1)$$

$$\delta^{18}Op = 0.973 \cdot \delta^{18}Oc\ (\pm 0.014) - 8.121\ (\pm 0.363)\ (n=59) \quad (2)$$

The two equations have identical slopes but Eqn. 1 has a significantly lower intercept than Eqn. 2. It is difficult to know

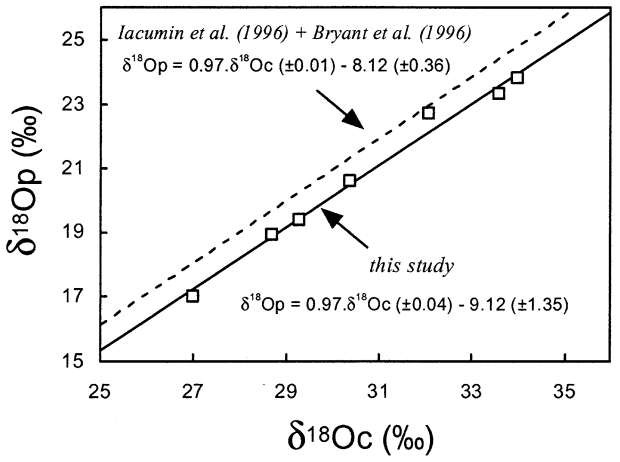

Fig. 1. Oxygen isotope compositions of phosphate ($\delta^{18}Op$) reported as a function of carbonate in apatite ($\delta^{18}Oc$) from modern hippopotamus tooth enamel. The solid line corresponds to the reduced major axis regression through all of the samples analyzed in this study. The dashed line shows a reduced major axis regression through results from the compiled data of Bryant et al. (1996) and Iacumin et al. (1996) obtained from modern mammals.

if this 1‰ shift results from differences between laboratory isotopic calibrations, or from specific physiologic properties of the hippopotamuses. Because the modern hippopotamus samples were prepared and run concurrently with our fossil samples, and because the slope of the equation that relates $\delta^{18}Op$ to $\delta^{18}Oc$ is the key parameter for the characterization of fossil apatite alteration (see "Discussion"), we will refer to regression line 1 for comparison with the fossil data. The average carbonate content in hippopotamus enamel is 3.9 ± 0.5 wt.%, identical to the carbonate content determined in previous studies (e.g., Rink and Schwarcz, 1995; Koch et al., 1997).

Oxygen isotope results and carbonate content measurements for fossil equids and bovids are given in Table 1. Fossil enamel and dentine show significant variations in their $\delta^{18}Oc$ and $\delta^{18}Op$ values. Oxygen isotope values in dentine are generally lower than in enamel from the same tooth, except for teeth TC24400 and TC23900 whose dentine samples have higher $\delta^{18}Oc$ values. Because these high $\delta^{18}Oc$ dentine samples do not have similarly high $\delta^{18}Op$ values, the isotope signatures likely reflect the precipitation of a secondary carbonate-bearing phase (probably carbonate apatite) that was not eliminated during the acetic acid pretreatment.

The slope of the equation that relates $\delta^{18}Op$ to $\delta^{18}Oc$ is close to one in modern apatite; thus, unaltered enamel is expected to have a similar isotopic range in both oxygen-bearing components. This is not the case for fossil enamels. Pliocene equid enamels from Chad exhibit isotopic ranges 0.5 to 0.8‰ higher in carbonate than in phosphate oxygen, whereas an opposite trend is observed for Miocene bovids from Greece and Afghanistan. Average individual carbonate contents of Greek and Afghan samples range from 3.4 to 4.6%, which matches the range measured in modern hippopotamus enamel (3.2–4.6%, Table 1) and other mammals (LeGeros and LeGeros, 1984; Rink and Schwarcz, 1995; Koch et al., 1997). In contrast, significant carbonate losses are noticed in the Chadian enamel samples, which have average carbonate contents between 2.2 and 3.0%.

4. DISCUSSION

4.1. Model Development

Laboratory experiments have demonstrated that microbially-mediated and inorganic exchange processes affect the oxygen isotope composition of carbonate and phosphate in different ways (Zazzo et al., 2004). In microbially-mediated reactions the oxygen isotope ratio of phosphate is modified more than that of carbonate; the opposite being observed during inorganic isotope exchange. This can be the result of different kinetics of isotopic exchange in the PO_4^{3-}-H_2O and CO_3^{2-}-H_2O systems as hypothesized by Iacumin et al. (1996), who observed that $\delta^{18}Oc$–$\delta^{18}Op$ couples measured in fossil apatites are often out of equilibrium and plot either below or above the equilibrium line. This can also be the result of the dissolution of primary apatite followed by the recrystallisation of secondary (diagenetically altered) apatite as suggested by Kolodny et al. (1996) amongst others. In this section, we present two models that describe the effect of inorganic and microbial diagenesis on the oxygen isotope compositions of fossil apatites.

4.1.1. Modeling Inorganic Diagenesis

The relative kinetics of isotopic exchange in the PO_4^{3-}-H_2O and CO_3^{2-}-H_2O systems are modeled within $\delta^{18}Oc$–$\delta^{18}Op$ space, adapted from the open system fluid-rock exchange model developed by Gregory and Criss (1986). The kinetics of isotopic exchange between phosphate and water or carbonate and water are described by

$$f = 1-\exp-(kt) = \frac{\delta^{18}O_{(i)}-\delta^{18}O_{(t)}}{\delta^{18}O_{(i)}-\delta^{18}O_{(e)}} \quad (3)$$

where f is the fraction of isotopic exchange between mineral and fluid, $\delta^{18}O_{(i)}$ is the initial oxygen isotope composition at $t = 0$, $\delta^{18}O_{(t)}$ is the composition measured at any time t, $\delta^{18}O_{(e)}$ is the composition at equilibrium, and k is the rate constant of the reaction. Two equations similar to Eqn. 3 are written, one for k_p, the rate constant of the PO_4^{3-}-H_2O system and the other for k_c, the rate constant of the CO_3^{2-}-H_2O system. For fluid buffered open systems, these two equations can be rearranged in exponential form to eliminate t so that the formulae become:

$$1-f_c = (1-f_p)^{k_c/k_p} \quad (4)$$

where f_c and f_p are the fractions of isotopic exchange for the CO_3^{2-}-H_2O and the PO_4^{3-}-H_2O systems, respectively.

This kinetic model can be applied without having prior knowledge of the mechanism of isotopic exchange. Inorganic diagenesis is equivalent to $k_p \ll k_c$. This model is applicable to fossil hypsodont teeth because they contain both carbonate and phosphate oxygen, and preserve short-term $\delta^{18}O$ variations corresponding to environmental variability during the time of tooth growth (Koch et al., 1989; Fricke and O'Neil, 1996). I, II, and III (Fig. 2) are the initial $\delta^{18}O$ values of either enamel or dentine samples from a given hypsodont tooth plotted within a $\delta^{18}Oc$–$\delta^{18}Op$ space. If the sample is completely reequilibrated

Table 1. Carbonate contents and oxygen isotope compositions of carbonate and phosphate of modern hippopotamus enamel, fossil enamel and dentine from Molayan (Afghanistan), Ravin des Zouaves (Greece) and Djurab (Chad).

N° sample	Locality	Tooth	Tissue	Position/EDJ (mm)	CO_3^{2-} (%)	$\delta^{18}Oc$ (SMOW, ‰)	$\delta^{18}Op$ (SMOW, ‰)
Modern African hippos (*Hippopotamus amphibius*)							
HA500	Dem. Rep. of Congo	C^1	Enamel	—	3.9	33.6	23.3
HA700	Dem. Rep. of Congo	M^1	Enamel	—	4.5	32.1	22.7
HA1000	Dem. Rep. of Congo	M^1	Enamel	—	3.6	28.7	18.9
HA1500	Dem. Rep. of Congo	P^4	Enamel	—	3.7	29.3	19.4
HA2500	Congo	P_3	Enamel	—	4.1	27.0	17.0
HA3100	Tanzania	P^3	Enamel	—	4.6	34.0	23.8
HA5400	Cameroon	C^1	Enamel	—	3.2	30.4	20.6
Miocene bovid (*Tragoportax* sp.) from Afghanistan (6.5–7.5 Ma)							
Mol311-7	Molayan	M_3	Enamel	03–06	3.6	33.0	23.5
Mol311-5			Enamel	09–11	3.9	32.4	23.0
Mol311-3			Enamel	15–19	3.9	29.3	19.3
Mol311-1			Enamel	22–27	3.8	27.5	17.3
Mol311			Enamel	Average	3.9		
Mol708-10	Molayan	M_3	Enamel	00–05	3.8	28.0	17.5
Mol708-9			Enamel	05–08	3.6	29.2	18.7
Mol708-4			Enamel	18–20	3.3	30.3	20.6
Mol708-1			Enamel	24–28	3.1	28.8	18.5
Mol708			Enamel	Average	3.4		
Mol271-9	Molayan	M_3	Enamel	00–03	4.3	29.8	20.1
Mol271-6			Enamel	07–09	4.0	30.8	21.9
Mol271-5			Enamel	09–11	4.3	31.8	23.4
Mol271-3			Enamel	14.5–16	4.0	32.5	23.6
Mol271-1			Enamel	19.5–23	4.0	30.4	20.4
Mol371			Enamel	Average	4.1		
Mol271-d3			Dentine	Lower	3.5	24.8	—
Mol271-d2			Dentine	Middle	3.2	25.8	—
Mol271-d1			Dentine	Upper	2.8	26.2	15.5
Miocene bovid (*Tragoportax* sp.) from Greece (6.5–7.5 Ma)							
RZO317-7	Ravin des Zouaves	M_3	Enamel	00–03	4.0	30.8	22.4
RZO317-6			Enamel	03–07	4.4	29.6	21.9
RZO317-5			Enamel	07–11	4.4	29.1	21.5
RZO317-4			Enamel	11–15	4.5	28.7	20.7
RZO317-3			Enamel	15–19	5.0	27.1	18.9
RZO317-2			Enamel	19–24	5.0	26.7	17.0
RZO317-1			Enamel	24–28	4.9	25.9	15.5
RZO317			Enamel	Average	4.6		
RZO317-d3			Dentine	Lower	4.4	24.8	15.1
RZO317-d2			Dentine	Middle	4.1	24.6	—
RZO317-d1			Dentine	Upper	4.0	24.4	—
Pliocene equid (*Hipparion* sp.) from Chad (5.5–3.5 Ma)							
TC24600-1	Koro Toro	P_2	Enamel	00–05	2.3	33.3	22.1
TC24600-3			Enamel	08–12	2.5	32.0	20.5
TC24600-5			Enamel	15–18	2.4	30.2	19.3
TC24600-7			Enamel	21–26	2.7	29.8	19.5
TC24600-9			Enamel	29–33	2.5	30.5	19.8
TC24600-11			Enamel	37–40	2.3	30.8	19.9
TC24600-14			Enamel	46–50	2.6	30.2	19.7
TC24600			Enamel	Average	2.5		
TC24600-d3			Dentine	Lower	1.8	29.6	18.3
TC24600-d2			Dentine	Middle	1.6	28.6	17.8
TC24600-d1			Dentine	Higher	1.6	29.1	18.1
TC24400-1	Kollé	M_3	Enamel	00–04	2.0	27.9	19.1
TC24400-5			Enamel	17–22	1.9	28.7	19.7
TC24400-10			Enamel	38–40	2.2	29.2	19.7
TC24400-12			Enamel	45–50	2.4	27.3	18.6
TC24400			Enamel	Average	2.2		
TC24400-d3			Dentine	Lower	2.0	28.5	19.0
TC24400-d2			Dentine	Middle	1.8	31.6	17.7
TC24400-d1			Dentine	Higher	1.6	33.1	17.7
TC23900-1	Kossom Bougoudi	P^2	Enamel	00–04	2.7	29.2	20.1
TC23900-4			Enamel	12–16	2.5	30.6	21.4
TC23900-6			Enamel	20–24	2.5	31.6	21.8
TC23900-9			Enamel	33–37	2.2	30.3	21.0
TC23900			Enamel	Average	2.5		
TC23900-d3			Dentine	Lower	1.4	27.1	17.3
TC23900-d2			Dentine	Middle	1.6	28.1	19.0
TC23900-d1			Dentine	Higher	2.2	34.6	18.6
TC23400-1	Kossom Bougoudi	M_3	Enamel	00–06	2.6	32.5	20.7
TC23400-2			Enamel	06–11	2.9	33.6	21.7
TC23400-6			Enamel	26–30	3.2	33.3	21.4
TC23400-9			Enamel	41–45	3.0	33.1	21.5
TC23400			Enamel	Average	3.0		
TC23400-d3			Dentine	Lower	1.3	28.6	18.0
TC23400-d2			Dentine	Middle	1.6	29.0	18.1
TC23400-d1			Dentine	Higher	1.7	28.0	19.0

Abbreviations: uppercase letters, upper teeth; lowercase letters, lower teeth; P, premolar; M, molars; C, canine. EDJ, enamel-dentine junction.

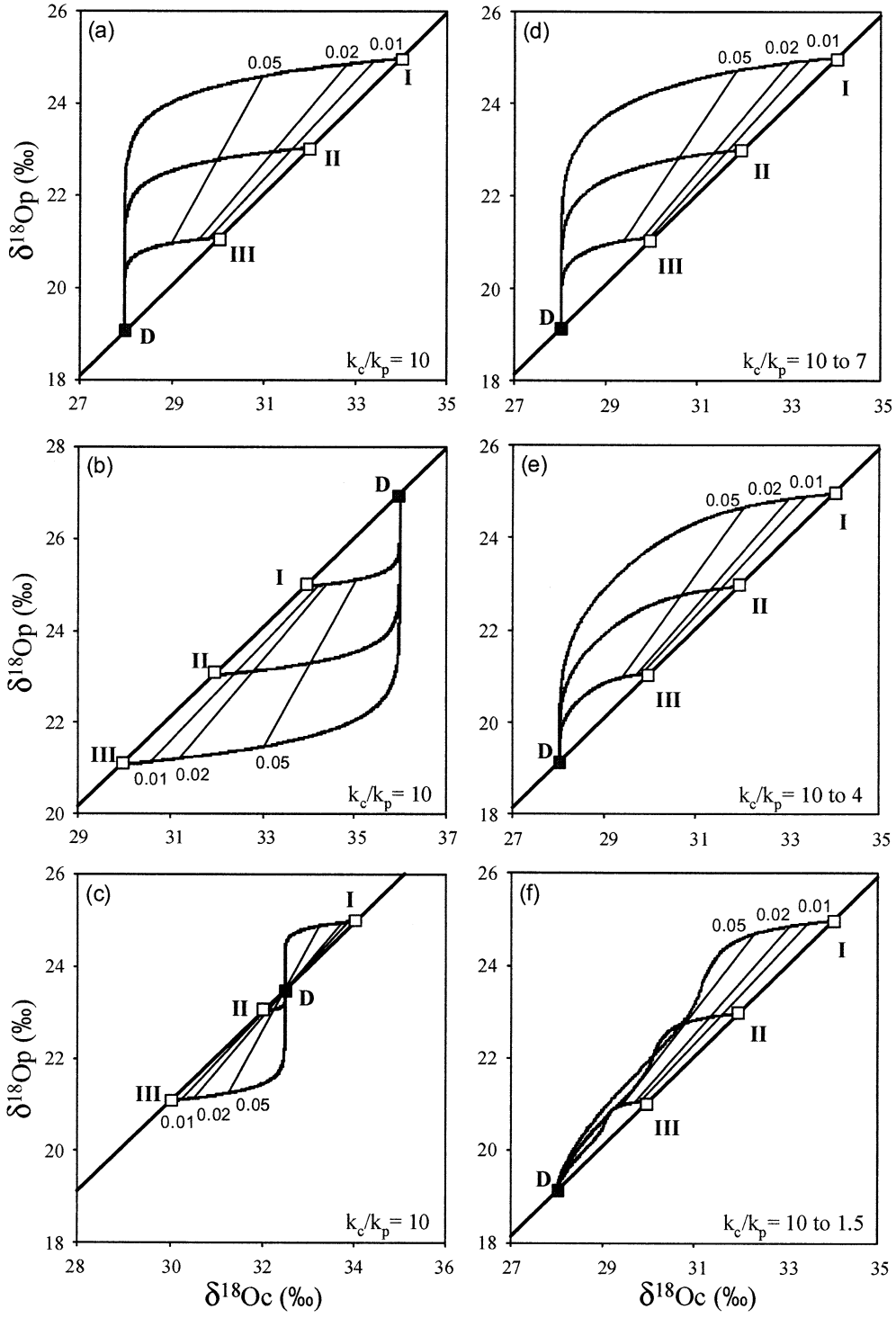

Fig. 2. Numerical simulation of exchange trajectories in δ^{18}Op–δ^{18}Oc space using the kinetic model assuming constant (a–c) and decreasing (d–f) k_c/k_p ratios. Along a single exchange-trajectory, samples that plot farthest from the initial point I, II, or III (open squares) have suffered the highest degree of alteration. The oxygen isotope composition of end-member D (filled square) can be lower (a, d–f), higher (b) or within the range of I to III values (c). The numbers represent constant f_p values. Note that as the paths approach D with increasing rates of isotopic exchange (or recrystallization), the intraindividual variability decreases.

with the diagenetic fluid, its composition will reach point D, following the path shown by the individual curve for that sample. Each set of curves represents the modeled exchange trajectories while the straight lines are lines of constant f_c and f_p values (Eqn. 3; Gregory and Criss, 1986). The oxygen isotope composition of a 100% re-equilibrated apatite can be

lower (Figs. 2a and 2d–2f), higher (Fig. 2b) or within the range (Fig. 2c) of unaltered apatite, depending on the oxygen isotope composition of the interacting fluid. We emphasize that case-studies presented in Figures 2a and 2d to 2f illustrate most cases of diagenetically-altered bioapatites (bone, dentine) that are generally depleted in ^{18}O compared to their initial isotopic compositions (e.g., Sharp et al., 2000). The curves are drawn for constant (Figs. 2a–2c) and decreasing (Figs. 2d–2f) k_c/k_p ratios through time, respectively. Decreasing k_c values (as a linear function of f) allow to account for the fact that the specific surface area available for oxygen isotope exchange between carbonate and water is likely to decrease during the course of the diagenetic process as a result of decreasing porosity and increasing crystal size. Although different trajectories can be generated, both case-scenarios lead to a similar conclusion, namely that slopes (A) are always higher than unity as a result of greater alteration of carbonate oxygen during inorganic diagenetic processes.

4.1.2. Modeling Microbial Diagenesis

Because P-O bonds are very resistant to breakage at low temperatures, especially in the solid-state, it is usually assumed that selective alteration of the oxygen isotope composition of biogenic phosphate requires first the dissolution of primary apatite followed by the microbially-mediated reprecipitation of a secondary apatite (Kolodny et al., 1996). Application of a kinetic model is less well suited to describe microbial diagenesis because oxygen isotope equilibrium between dissolved phosphate ions and water is rapidly promoted by microbial activity (Blake et al., 1997), and one can assume that both the CO_3^{2-}-H_2O and the PO_4^{3-}-H_2O systems reach oxygen isotope equilibrium instantaneously ($k_p \approx k_c \gg 0$). Instead, microbially-mediated diagenesis is best modeled using simple mass-balance equations. If one assumes that the temperature and isotopic composition of the diagenetic fluid are constant during the exchange process, and that dissolved carbonate and phosphate reach equilibrium with the water, then one can consider that a partly recrystallised apatite sample is composed of a mixture of two end-members (1) the unexchanged fraction with its initial $\delta^{18}O$ value, and (2) the completely exchanged fraction. This can be expressed as follows:

$$\delta^{18}O_f = \frac{C_{II} \cdot X \cdot \delta^{18}O_{eq} + C_I \cdot (1-X) \cdot \delta^{18}O_i}{C_{syst}} \qquad (5)$$

where $\delta^{18}O_i$ and $\delta^{18}O_f$ are the oxygen isotope compositions of enamel before and after alteration, X and $\delta^{18}O_{eq}$ are the proportion and the oxygen isotope composition of secondary apatite at equilibrium with the diagenetic aqueous fluids, and C_I, C_{II} and C_{syst} are the concentrations of oxygen in the biogenic apatite, the secondary apatite and the fossil, respectively. Two equations similar to Eqn. 5 can be written, one for $\delta^{18}Op$, and the other for $\delta^{18}Oc$. This model can readily account for the fact that primary and secondary apatites may have different CO_3^{2-}/PO_4^{3-} ratios. This ratio is controlled mainly by the amount of carbonate in apatite since $[CO_3^{2-}] \ll [PO_4^{3-}]$. The curves in Figure 3a are drawn for different extents of recrystallisation (X values) considering a lower CO_3^{2-}/PO_4^{3-} ratio in secondary apatite than in biogenic apatite, in the range observed for

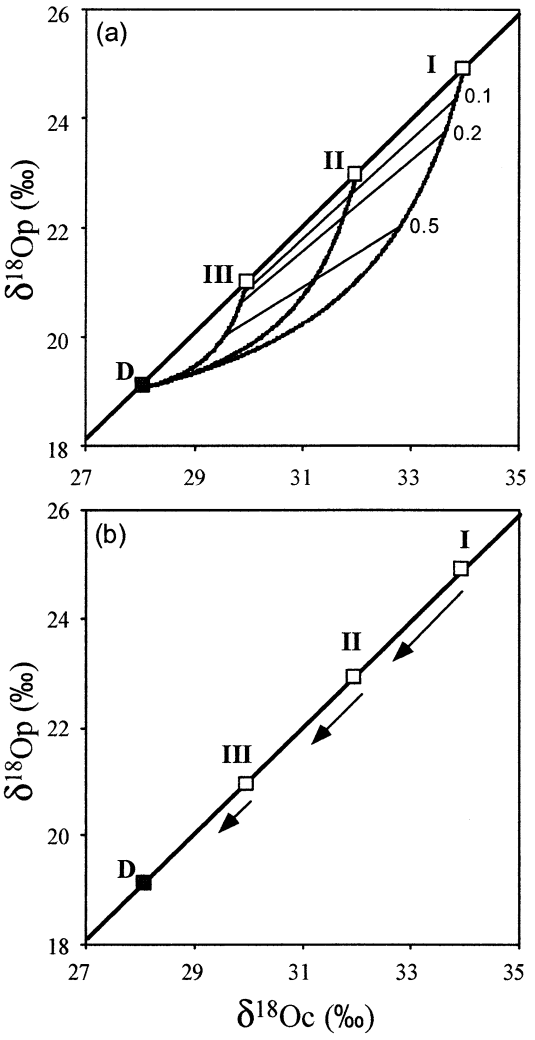

Fig. 3. Numerical simulation of exchange trajectories in $\delta^{18}Op$–$\delta^{18}Oc$ space using the mass-balance model. The numbers represent the extent of recrystallization (X). The curves in (a) are drawn assuming that the secondary apatite contain four times less carbonate than the primary apatite. In (b) CO_3^{2-}/PO_4^{3-} ratios are similar in primary and secondary apatites and exchange trajectories slide along the equilibrium line, as indicated by the arrows. Note that as the paths approach D with increasing rates of recrystallization, the intraindividual variability decreases.

natural and experimental carbonate fluorapatites (Jahnke, 1984). In the case of similar CO_3^{2-}/PO_4^{3-} ratios for the primary and secondary apatites, the $\delta^{18}Oc$–$\delta^{18}Op$ couples will slide along the equilibrium line (Fig. 3b). Therefore, slopes (A) can be equal or lower than unity depending on the carbonate content of the secondary apatite. Slopes lower than unity imply that there was a higher rate of isotopic exchange for phosphate oxygen than for carbonate oxygen, which we interpret as the result of microbially-mediated reactions. Slopes equal to unity can be used as evidence for the preservation of both $\delta^{18}Oc$ and $\delta^{18}Op$ values only if recrystallisation did not occurred.

According to our models, sequential analyses in fossil hypsodont teeth have the potential (1) to discriminate between inorganic and microbially-mediated diagenetic alteration, and

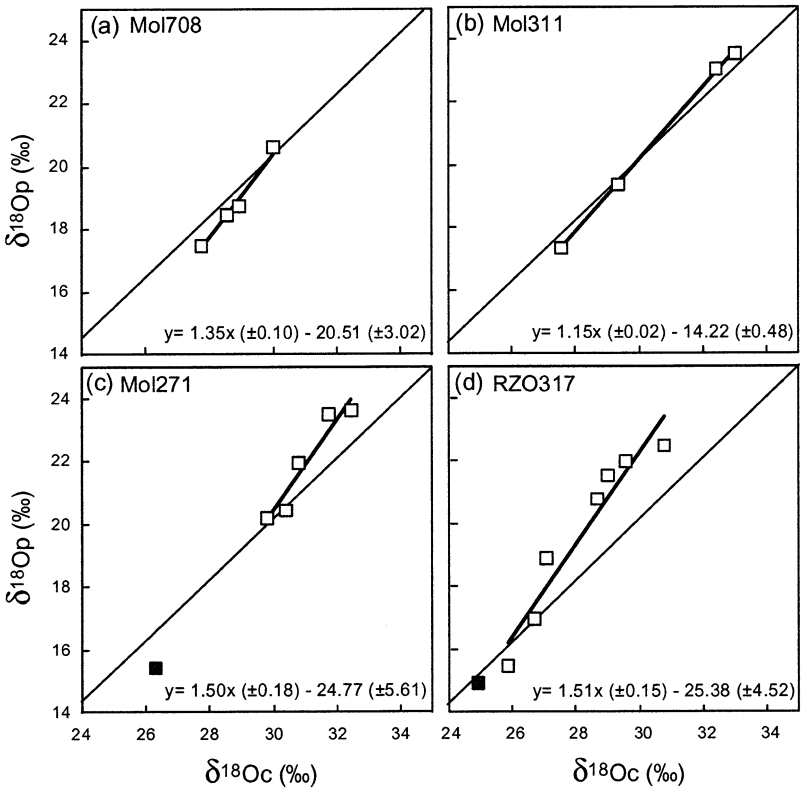

Fig. 4. Intratooth oxygen isotope compositions of phosphate ($\delta^{18}Op$) reported as a function of the oxygen isotope composition of carbonate ($\delta^{18}Oc$) in late Miocene bovid (*Tragoportax* sp.) from Molayan, Afghanistan (a–c) and Ravin des Zouaves, Greece (d) (dentine: filled squares; enamel: open squares). Slopes (*A*) higher than unity are calculated for each tooth enamel. Water-apatite interaction under inorganic conditions appears to be the dominant process during the diagenesis of fossil enamel, whereas low $\delta^{18}Op$ values of dentines indicate diagenesis under microbial conditions.

(2) to provide constraints on the oxygen isotope composition of the diagenetic end-member.

4.2. Application to Fossil Teeth

4.2.1. Inorganic and Microbial Diagenesis

Bovid enamel from the Miocene sites of Molayan (Afghanistan) and Ravin des Zouaves (Greece) show *A* values that are systematically higher than unity (Fig. 4). Slopes and intercepts differ significantly (*t* test, $p < 0.001$) from that calculated from modern enamel. These results indicate that the fossil enamels underwent diagenetic changes that were driven by inorganic processes. Greek and Afghan data sets plot across the PO_4^{3-}-CO_3^{2-} reference line, with the lowest value below and the highest value above the line, which corresponds to the theoretical case-study described in Figure 2c. According to our model, the point at which the data trend crosses the equilibrium line is the inferred value of the diagenetic end-member. This result suggests that the $\delta^{18}Oc$ value of a 100% re-equilibrated apatite is within the range 26 to 27‰ in Ravin des Zouaves and 30 to 31‰ in Molayan. Dentine samples give the best estimate for the completely diagenetically modified bioapatite with $\delta^{18}Oc$ values between 24 and 26‰, and $\delta^{18}Op$ values between 15 and 16‰ in both sites. The Greek data set is in good agreement with the predictions of the model, indicating that enamel and dentine in apatite interacted with the same diagenetic aqueous fluid. On the contrary, the $\delta^{18}Oc$ and $\delta^{18}Op$ values found in Afghan dentine are ~4‰ lower than the diagenetic end-member inferred from the enamel data trends. This result raises the possibility of multi-stage alteration for Afghan teeth, i.e., early (rapid) stage of microbial and inorganic diagenesis with ^{18}O-depleted water (relative to SMOW) in dentine; and later inorganic (slow) oxygen isotope exchange between carbonate in enamel apatite and a different (^{18}O-enriched) water.

Equid enamel from the Pliocene sites of Chad show *A* values that are systematically lower than unity (Fig. 5). All intercepts and all slopes but one (TC23400) differ significantly ($p < 0.001$) from that measured in modern enamel. This result indicates that for at least three specimens, enamel diagenesis took place under microbial mediation and that phosphate oxygen underwent isotopic exchange with aqueous fluids. The $\delta^{18}Op$ values are lower in dentine than in enamel, and probably reflect more extensive interaction between dentine and water during the early stage of microbial diagenesis. The dentine samples from teeth TC24600 and TC23400 plot close to the reference line, and are considered as best estimates of samples that isotopically reequilibrated with the diagenetic aqueous fluids. Carbonate in apatite is ^{18}O-enriched relative to the expected equilibrium value in some dentine samples that plot to the right of the reference line, indicating that the dentine may have recorded a second diagenetic event that selectively modified the oxygen isotope compositions of carbonate in apatite.

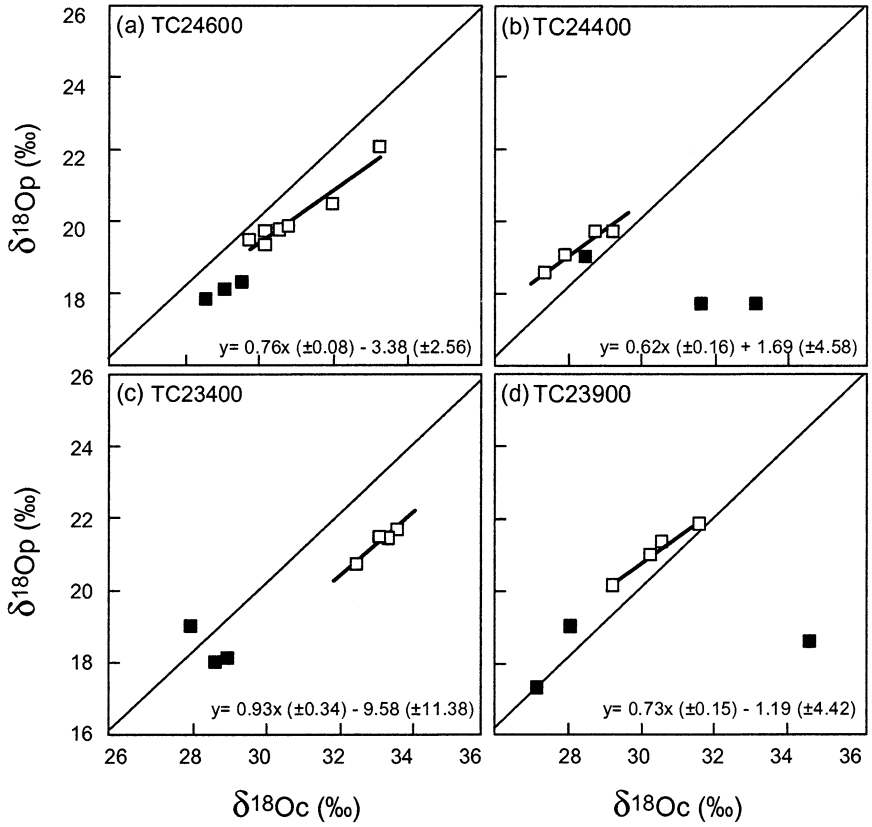

Fig. 5. Intratooth oxygen isotope compositions of phosphate (δ^{18}Op) reported as a function of the oxygen isotope composition of carbonate (δ^{18}Oc) in Pliocene equids (*Hipparion* sp.) from Djurab, Chad (dentine: filled squares; enamel: open squares). Slopes (*A*) lower than unity are calculated for each tooth enamel. Water-apatite interaction under microbial mediation appears to be the dominant process during the diagenesis of fossil enamel and dentine.

Until the early 1990s, δ^{18}Op values of fossil material were generally accepted as primary values (Kolodny and Luz, 1991; Barrick and Showers, 1994, 1995; Barrick et al., 1996). However, the study of Shemesh (1990) on sedimentary apatites, which described changes in δ^{18}Op associated with recrystallization, led several authors to examine the evidence for isotopic exchange between fossil bone or dentine and its surrounding fluids during early diagenesis (e.g., Ayliffe et al., 1994; Sharp et al., 2000). As far as we know, this is the first time that isotopic exchange between phosphate and water is clearly demonstrated in fossil enamel.

4.3. Correction of Diagenetic Effects Recorded in Fossil Enamel

4.3.1. Identification of the Mechanisms of Diagenetic Alteration

The occurrence of two populations of slopes for fossil bovids and equids suggests that enamel oxygen isotope compositions were modified by two different diagenetic processes. Small-sized bone crystallites are sensitive to recrystallization and are consequently highly susceptible to postmortem exchange. Increases in the average size of apatite crystallites can be monitored with X-ray diffractometry or infra-red spectroscopy (Tuross et al., 1989; Ayliffe et al., 1994; Michel et al., 1995; Person et al., 1995) and can be quantified by the crystallinity index (CI index). Recrystallization is generally well correlated to chemical changes like increasing fluoride contents or decreasing carbonate contents, which improve the stability of the apatite crystals (Shemesh, 1990; Kohn et al., 1999; Balter, 2001). Fluoride and carbonate contents have, therefore, been used as indirect indicators of apatite recrystallization (Shemesh, 1990) and bone/enamel diagenesis (Bryant et al., 1994).

In our Greek and Afghan samples, for which only inorganic isotope exchange is thought to have occurred, there is no significant relationship between A, which is a proxy for the extent of isotopic exchange in the carbonate fraction, and the average carbonate content [CO_3^{2-}] of the enamel (r^2 = 0.30 ; Fig. 6). Moreover, [CO_3^{2-}] is very similar to that measured in modern enamel. There is no clear evidence of recrystallization in these fossils. Isotopic alteration of carbonate without recrystallization suggests that the alteration is occurring via exchange of oxygen between the fluid and the solid bioapatite probably by diffusion (see section 4.1.1). This scenario accounts for the fact that carbonate isotope alteration is never pervasive in enamel, but is commonly extensive in the more porous bone and dentine, which are only a few unit cells thick, and have nearly all the carbonate ions available for exchange.

In Chad, isotopic exchange between phosphate and water

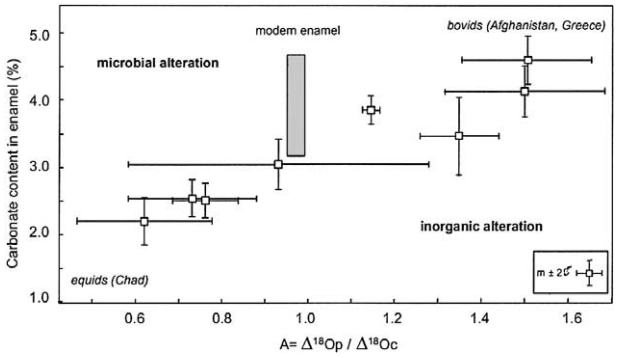

Fig. 6. Relationship between the average carbonate content and the slope (*A*) measured in enamel of *Hipparion* sp. (Chad) and of *Tragoportax* sp. (Afghanistan). Average values and standard deviations are indicated for each tooth. The grey area defines the slope and range of measured carbonate contents in modern enamel. Slopes lower than unity are correlated to the carbonate content in fossil equid from Chad, whereas no apparent correlation is observed between slopes higher than unity and carbonate contents in Afghan and Greek bovid enamels.

was clearly linked to enamel recrystallization. The extent of $\delta^{18}Op$ resetting, approximated by *A* values, is related to the carbonate content. Reduced major axis regression yields the following empirical relationship:

$$[CO_3^{2-}] = 2.68 \cdot A(\pm 0.15) + 0.52\ (\pm 0.12)(r^2 = 0.99) \quad (6)$$

For unaltered enamel ($A = 1$), $[CO_3{}^{2-}] = 3.2\%$, which corresponds to the lowest value measured amongst modern (non altered) hippopotamuses. Solving Eqn. 6 for $A = 0$ gives the carbonate content of the secondary mineralized apatite corresponding to the oxygen isotope compositions of phosphate totally reequilibrated with the reacting water. This apatite has essentially no carbonate, as hypothesized in our dissolution-reprecipitation model (see section 4.1.2). Zazzo (2001) has shown that in several fossil enamel and dentine samples from Chad, the decrease in carbonate is paired to an increase in fluoride content. It is, therefore, likely that the secondary apatite is a carbonate fluorapatite, the more stable end-member of the apatite family. This result is in keeping with those obtained by Shemesh (1990) and Soudry and Nathan (2000) in phosphorites, and enforces the assumption made by Kolodny et al. (1996) that "practically all apatitic fossils consist of carbonate-fluor apatite as the major mineral phase in contrast to the biologic apatite" and that diagenesis "occurs by dissolution-reprecipitation." Moreover, our results indicate that this replacement is probably microbially-mediated.

The relative proportion of secondary apatite (*X*) can be estimated by using the following equation:

$$X = \frac{([CO_3^{2-}]_i - [CO_3^{2-}]_{mes}) \cdot 100}{[CO_3^{2-}]_i} \quad (7)$$

where $[CO_3{}^{2-}]_i$ is the carbonate content of modern enamel and $[CO_3{}^{2-}]_{mes}$ is the measured carbonate content of fossil enamel. It is relatively difficult to assign a value for $[CO_3{}^{2-}]_i$ because of the wide range of carbonate content observed in modern mammal enamel. Solving Eqn. 6 for $A = 1$ gives $[CO_3{}^{2-}]_i = 3.2\%$, similar to average human enamel carbonate content (Driessens and Verbeeck, 1990). Applying Eqn. 7 to fossil equids indicates that CFA could constitute 5.6 ± 0.2% to 31.6 ± 1.4% of the whole fossil enamel (Table 2). However, the value of 3.2% for modern enamel should be considered as a threshold for detecting recrystallization. A more pessimistic scenario, using the average hippopotamus carbonate content indicates that CFA could constitute from 22.6 ± 0.7% to 43.8 ± 2.0% of the fossil enamels (Table 2).

4.3.2. Correcting for Inorganic Diagenesis

During inorganic oxygen isotope exchange at surface temperatures, only the carbonate oxygen will exchange with oxygen from ambient water because of very slow kinetics between phosphate oxygen and water at Earth surface temperature (Lécuyer et al., 1999; Zazzo et al., 2004). In Afghan and Greek fossil enamels, the average carbonate content did not change (and would have decreased in case of fluorapatite addition) indicating that secondary precipitation of diagenetic apatite did not occur. Oxygen isotope compositions of phosphate can, therefore, be considered close to pristine reflections of the isotopic composition of the mammal body water. Restoration of original $\delta^{18}Oc$ values can be performed for each enamel sample by introducing the $\delta^{18}Op$ value of each sample into the carbonate-phosphate equation determined for modern mammals. Corrected $\delta^{18}Oc$ values are 0.7‰ lower to 2.3‰ higher than the measured values, and the intratooth range is 0.9 to 2.1‰ higher after correction (Table 2).

4.3.3. Correcting for Microbial Diagenesis

In the case of enamel diagenesis operating under microbial mediation, the correction requires a step by step protocol because both $\delta^{18}Oc$ and $\delta^{18}Op$ values may be altered. Low slopes show that phosphate oxygen isotopes were more extensively exchanged than those from carbonate in apatite. The extent of isotopic alteration is positively correlated to the amount of secondary apatite precipitated in fossil enamel, as expressed in Eqn. 5. Eqn. 5 can be rearranged to isolate $\delta^{18}Op_i$:

$$\delta^{18}Op_i = \frac{-X \cdot \delta^{18}Op_{eq} + \delta^{18}Op_f}{(1-X)} \quad (8)$$

$\delta^{18}Op_f$ is measured and *X* can be estimated using Eqn. 7. The only parameter that remains undetermined so far is $\delta^{18}Op_{eq}$. Because enamel and dentine from the same tooth share the same diagenetic history, and because dentine is more extensively exchanged than enamel, $\delta^{18}O$ values in dentine can serve as a proxy of the $\delta^{18}O$ value of secondary apatite that recrystallized in equilibrium with the diagenetic fluid. $\delta^{18}Op$ values are preferred to $\delta^{18}Oc$ values because the diagenetic overprint of the phosphate component is obtained during early diagenesis through bacterial degradation of organic matter. In contrast, carbonate oxygen may be sensitive to inorganic isotope exchange with another aqueous fluid via a late diagenetic event.

For the Chad samples, low $\delta^{18}Op$ values of dentine indicate that the diagenetic fluid is ^{18}O-depleted compared to mammalian body water that is in equilibrium with biologic

Table 2. Calculated secondary apatite content (X_1 to X_3) and initial $\delta^{18}O$ values ($\delta^{18}O_{calculated}$) in fossil enamel assuming different initial carbonate contents $[CO_3^{2-}]_i$. Measured and calculated $\delta^{18}O$ values are indicated for the carbonate fraction (Afghanistan, Greece) and phosphate fraction (Chad), respectively. Corrections in Greek and Afghan enamel are estimated using the carbonate-phosphate equation of Shemesh (1988), assuming that phosphate $\delta^{18}O$ values are unaltered; corrections in Chad enamel are estimated using Eqn. 8, assuming that dentine values are 100% re-equilibrated with the diagenetic aqueous fluid. The result of error propagation calculations ($\pm 1\sigma$) are indicated for X and $\delta^{18}Op_{calc}$ values.

N° LBI	X_1 (%) $[CO_3^{2-}]_i = 3.2\%$	X_2 (%) $[CO_3^{2-}]_i = 3.5\%$	X_3 (%) $[CO_3^{2-}]_i = 3.9\%$	$\delta^{18}O$ measured (SMOW ‰)	$\delta^{18}O$ calculated (SMOW ‰)		
Molayan, Afghanistan				Carbonate fraction			
Mol311	0	0	0				
Mol311-1				27.5	27.1		
Mol311-3				29.3	29.2		
Mol311-5				32.4	33.0		
Mol311-7				33.0	33.5		
Mol708	0	0	0				
Mol708-1				28.8	28.4		
Mol708-4				30.3	30.5		
Mol708-9				29.2	28.6		
Mol708-10				28.0	27.3		
Mol271	0	0	0				
Mol271-1				30.4	30.3		
Mol271-3				32.5	33.6		
Mol271-5				31.8	33.4		
Mol271-6				30.8	31.8		
Mol271-9				29.8	30.0		
Ravin des Zouaves, Greece							
RZO317-1				25.9	25.3		
RZO317-2				26.7	26.8		
RZO317-3				27.1	28.7		
RZO317-4				28.7	30.7		
RZO317-5				29.1	31.4		
RZO317-6				29.6	31.9		
RZO317-7				30.8	32.4		
RZO317	0	0	0				
Djurab, Chad				Phosphate fraction			
					$[CO_3^{2-}]_i = 3.2\%$	$[CO_3^{2-}]_i = 3.5\%$	$[CO_3^{2-}]_i = 3.9\%$
TC24600	21.9 ± 0.9	28.6 ± 1.1	35.9 ± 1.4				
TC24600-1				22.1	23.3 ± 1.0	23.8 ± 1.0	24.5 ± 1.1
TC24600-3				20.5	21.3 ± 0.9	21.6 ± 0.9	22.0 ± 1.0
TC24600-5				19.3	19.7 ± 0.9	19.9 ± 0.9	20.1 ± 0.9
TC24600-7				19.5	20.0 ± 0.9	20.2 ± 0.9	20.5 ± 1.0
TC24600-9				19.8	20.4 ± 0.9	20.6 ± 0.9	20.9 ± 1.0
TC24600-11				19.9	20.5 ± 0.9	20.7 ± 0.9	21.1 ± 0.9
TC24600-14				19.7	20.2 ± 0.9	20.5 ± 0.9	20.8 ± 0.9
TC24400	31.6 ± 1.4	37.4 ± 1.7	43.8 ± 2.0				
TC24400-1				19.1	19.8 ± 1.0	19.9 ± 1.1	20.2 ± 1.2
TC24400-5				19.7	20.6 ± 1.0	20.9 ± 1.1	21.3 ± 1.2
TC24400-10				19.7	20.6 ± 1.0	20.9 ± 1.1	21.3 ± 1.2
TC24400-12				18.6	19.0 ± 1.0	19.1 ± 1.1	19.3 ± 1.2
TC23900	21.6 ± 0.9	28.3 ± 1.1	35.6 ± 1.4				
TC23900-1				20.1	20.9 ± 1.0	21.3 ± 0.9	21.7 ± 0.8
TC23900-4				21.4	22.5 ± 1.0	23.1 ± 1.0	23.7 ± 0.9
TC23900-6				21.8	23.0 ± 1.0	23.7 ± 1.0	24.3 ± 0.9
TC23900-9				21.0	22.0 ± 1.0	22.6 ± 1.0	23.1 ± 0.8
TC23400	5.6 ± 0.2	13.7 ± 0.5	22.6 ± 0.7				
TC23400-1				20.7	20.9 ± 0.8	21.1 ± 0.8	21.5 ± 0.7
TC23400-2				21.7	21.9 ± 0.8	22.3 ± 0.9	22.8 ± 0.7
TC23400-6				21.4	21.6 ± 0.8	21.9 ± 0.8	22.4 ± 0.8
TC23400-9				21.5	21.7 ± 0.8	22.1 ± 0.8	22.5 ± 0.8

apatites. The range of apatite $\delta^{18}Op$ values expected to form at isotopic equilibrium with environmental water from sub-Saharan Africa ($\delta^{18}Op_{eq}$) can be calculated. We used the phosphate-water fractionation equation of Shemesh et al. (1988) along with the mean annual temperature and oxygen isotope compositions of meteoric waters measured in Sudan, Mali, Chad and Nigeria by the IAEA/WMO (2001). Mean $\delta^{18}Op$ values indicate that a 100% reequilibrated apatite should lie between 15 and 17‰ in these sub-Saharan countries. These values are slightly lower than those measured in our dentine samples. Three reasons can be invoked to explain this result: (1) it is inappropriate to use mean temperature and meteoric water $\delta^{18}O$ value to characterize the diagenetic fluid; (2) climatic conditions in Chad were different during the Pliocene; (3) the reequilibration of dentine with diagenetic fluids was incomplete. Alteration might only

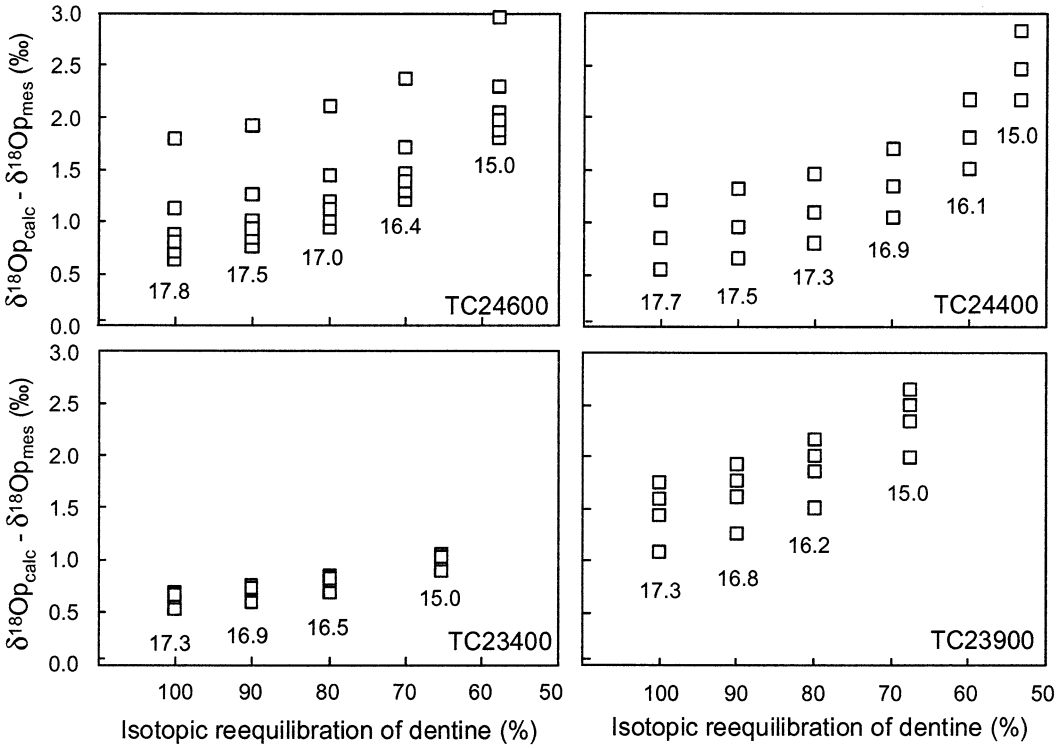

Fig. 7. Calculated shifts to fossil equid enamel $\delta^{18}Op$ values ($\delta^{18}Op_{calc} - \delta^{18}Op_{mes}$) vs. degree of isotopic reequilibration of dentine. The $\delta^{18}Op_{calc}$ values are calculated assuming $[CO_3^{2-}]_i = 3.5\%$. The different squares in a column correspond to individual subsamples from a single zoning profile. For each profile, calculated shifts differ from one another because subsample compositions are different. Each column assumes that the lowest measured $\delta^{18}Op$ value of dentine correspond to a different degree of isotopic reequilibration. The number below each column is the measured (for the first column) or the calculated composition of the diagenetic end-member based on the lowest dentine $\delta^{18}Op$ value. Errors (± 0.7–1.2‰, 1σ, Table 2) are not plotted on this figure.

occur during wet conditions, when temperature is generally lower, or in evaporated soil waters that have undergone ^{18}O-enrichment compared to mean annual precipitation. Also, climatic changes have probably affected northern Chad since the Pliocene. But these parameters are difficult to estimate precisely. On the other hand, the observation of 0.5‰ to 1.7‰ intraindividual $\delta^{18}Op$ variations in fossil dentine suggests that this tissue did not completely re-equilibrate with the diagenetic fluid. Because the $\delta^{18}O$ of mammalian body water is sufficiently enriched over local precipitation, alteration generally leads to lower $\delta^{18}Op$ values, so the lowest dentine $\delta^{18}Op$ value measured in each tooth should be considered as the best estimate of $\delta^{18}Op_{eq}$.

Correction formulae have to take into account this uncertainty. If we adapt Eqn. 5 to enamel (e) and dentine (d) phosphate, and considering $C_I = C_{II}$, we obtain

$$\text{enamel:}\delta^{18}Op_{E,f} = X_E \cdot \delta^{18}Op_{eq} + (1-X_E) \cdot \delta^{18}Op_{E,i} \quad (9)$$

$$\text{dentine:}\delta^{18}Op_{D,f} = X_D \cdot \delta^{18}Op_{eq} + (1-X_D) \cdot \delta^{18}Op_{D,i} \quad (10)$$

If Eqn. 10 is solved over the range $X_d = 0$ *to* 1, and $\delta^{18}Op_{d,i} > \delta^{18}Op_{eq}$, partial isotopic exchange with the aqueous fluid is shown to produce $\delta^{18}Op_{d,f}$ values that remain higher than $\delta^{18}Op_{eq}$ values. Figure 7 presents the correction of Chad enamel $\delta^{18}Op$ values as a function of the extent of isotopic reequilibration of dentine with the diagenetic fluid. $\delta^{18}Op_{eq}$ values associated with X_D values are calculated by combining Eqn. 9 and 10. In contrast to bones that grow and are reworked throughout the lifespan of an animal, enamel and dentine mineralizations take place early and relatively quickly, during approximately the same stage of ontogeny. Enamel and dentine of individual specimens are, therefore, expected to have similar mean isotopic compositions and we can assume that $\delta^{18}Op_{e,i} = \delta^{18}Op_{d,i}$. Hence, $\delta^{18}Op_{eq}$ is a function of X_e, X_d, $\delta^{18}Op_{e,f}$ and $\delta^{18}Op_{d,f}$ such that

$$\delta^{18}Op_{eq} = \frac{\delta^{18}Op_{D,f} \cdot (1-X_E) - \delta^{18}Op_{E,f} \cdot (1-X_D)}{X_E \cdot (1-X_D) - X_D \cdot (1-X_E)} \quad (11)$$

In the Chad samples, a $\delta^{18}Op_{eq}$ value of 15‰ is computed when 53 to 68% of dentine is isotopically exchanged with the diagenetic aqueous fluid (Fig. 7). The correction is variable within a tooth and is highest for samples with high $\delta^{18}Op$ values. If the lowest dentine $\delta^{18}Op$ value reflects $\delta^{18}Op_{eq}$ value, and assuming $[CO_3^{2-}]_i = 3.5\%$, corrected $\delta^{18}Op$ values in enamel are 0.5 to 1.8‰ higher than measured values. If dentine is partly re-equilibrated, these corrections may, locally, be as high as 3‰ (Fig. 7). After correction, intratooth ranges increase by 0.1 to 1.2‰ (Table 2).

There is no uncertainty in cases of inorganic alteration because $\delta^{18}Op$ values in enamel remain pristine. But when microbial alteration of fossil enamel is indicated, corrections

require accurate knowledge of (1) alteration intensity (*X* values), and (2) the oxygen isotope composition of water that reacted with the apatites. Calculations using the principles of error propagation indicate relatively high uncertainty, even when a value is assigned to $[CO_3^{2-}]_i$ (0.7–1.2‰, 1σ, Table 2). In addition, and because the δ^{18}Op value of fossil dentine may only reflect partial re-equilibration with reacting water, corrections using δ^{18}Op values of fossil dentine as a proxy for $\delta^{18}Op_{eq}$ must be considered as low estimates. Yet, because it is difficult to assign a value to $[CO_3^{2-}]_i$, a method allowing quantitatively precise estimate of the CFA content in fossil apatites remains to be found. Further studies will have to investigate whether microbial diagenesis of enamel is common at Earth surface conditions. Also, a better understanding of the kinetics and extent of oxygen isotope reequilibration in fossil enamel and dentine will be necessary to improve the quality of the corrections, and consequently, paleoenvironmental reconstructions.

5. CONCLUSIONS

This study provides the first evidence that the oxygen isotope composition of fossil enamel can be either inorganically or microbially-altered depending on the burial conditions. Modifications of the pristine oxygen isotope compositions of carbonate and phosphate in apatite can be identified in hypsodont enamel through a treatment of data in a δ^{18}Oc–δ^{18}Op space. In cases of inorganic alteration, no recrystallization is observed and only oxygen isotope compositions of carbonate in apatite are modified. In contrast, microbially-induced alteration is associated with extensive recrystallization of enamel apatite via a loss of carbonate, and isotopic exchange is observed in both carbonate and phosphate oxygen. Our results on Chadian fossils also suggest that the reliability of fossil enamel δ^{18}Op values can be easily tested via the measure of enamel carbonate content.

The main goal of climate reconstitutions is to detect and quantify both annual and seasonal oxygen isotope changes recorded in fossil apatites. Major climatic changes are characterized by mean air temperature variations of only a few degrees and are recorded in fossil apatites by δ^{18}O variations that rarely exceed 2‰. For example, during the Pleistocene, the shift from glacial to interglacial climate was recorded in proboscidean tusks from England, by a 1 to 2‰ difference in their δ^{18}Op values (Ayliffe et al., 1992). Patterns of seasonal variations in temperature or precipitation are sometimes more helpful for understanding the distribution of faunal communities on Earth. For example, sequential sampling and δ^{18}O analyses of North American fossil otoliths revealed that the Eocene-Oligocene transition was characterized by an increased seasonality while mean annual temperatures remained unchanged (Ivany et al., 2000).

It is essential to correct for postmortem oxygen isotope shifts recorded in diagenetic apatites to estimate accurately mean annual and seasonal temperature variation. Our study of Miocene-Pliocene fossils reveals that δ^{18}O changes due to diagenesis may locally exceed 2‰. These limited isotopic changes are difficult to detect through a comparison of δ^{18}Oc–δ^{18}Op bulk sample values, and sequential sampling has also shown that diagenesis can smooth out patterns of intraindividual oxygen isotope variations in the enamel carbonate and phosphate. As a result, the amplitudes of annual and seasonal climatic changes may be underestimated if diagenesis is not carefully diagnosed. Finally, it may be possible to correct for the isotopic effects resulting from a diagenetic alteration of biogenic apatites in some data sets, thus improving the quality of continental climatic reconstructions.

Acknowledgments—We would like to thank Michel Brunet and all the M.P.F.T. members for providing us with the hipparion teeth samples from Chad. Bovid teeth from Afghanistan and Greece were given by Emile Heintz, Sevket Sen and Louis de Bonis. Jean-Renaud Boisserie provided us with the modern hippopotamuse samples from Africa. We also would like to thank Michelle Emery and François Martineau for technical assistance. Sandy Bonny kindly improved the English of this manuscript. We also wish to thank Paul Koch, Matt Kohn, Juske Horita, Yuanming Pan and two anonymous reviewers for constructive criticism of an earlier version of this paper.

Associate editor: J. Horita

REFERENCES

Ayliffe L. K., Lister A. M., and Chivas A. R. (1992) The preservation of glacial interglacial climatic signatures in the oxygen isotopes of elephant skeletal phosphate. *Palaeogeogr. Palaeoclimatol. Palaeoecol.* **99,** 179–191.

Ayliffe L. K., Chivas A. R., and Leakey M. G. (1994) The retention of primary oxygen isotope composition of fossil elephant skeletal phosphate. *Geochim. Cosmochim. Acta* **58,** 5291–5298.

Balasse M. (2002) Reconstructing dietary and environmental history from enamel isotopic analysis: Time resolution of intra-tooth sequential sampling. *Int. J. Osteoarch.* **12,** 155–165.

Balasse M., Ambrose S. H., Smith A. B., and Price T. D. (2002) The seasonal mobility model for prehistoric herders in the south-western Cape of South Africa assessed by isotopic analysis of sheep tooth enamel. *J. Arch. Sci.* **29,** 917–932.

Balter V (2001) Les rapports Sr/Ca et Ba/Ca dans les phosphates biogéniques. Applications paléo-écologiques et paléo-anthropologiques. Ph.D. dissertation, Univ. Bordeaux I and Paris VI, Bordeaux.

Barrick R. E. and Showers W. J. (1994) Thermophysiology of *Tyrannosaurus rex*: Evidence from oxygen isotopes. *Science* **265,** 222–224.

Barrick R. E. and Showers W. J. (1995) Oxygen isotope variability in juvenile dinosaurs (*Hypacrosaurus*): Evidence for thermoregulation. *Paleobiology* **21,** 552–560.

Barrick R. E., Showers W. J., and Fischer A. G. (1996) Comparison of thermoregulation of four ornithischian dinosaurs and a varanid lizard from the Cretaceous Two Medicine Formation: Evidence from oxygen isotopes. *Palaios* **11,** 295–305.

Blake R. E., O'Neil J. R., and Garcia G. A. (1997) Oxygen isotope systematics of biologically mediated reactions of phosphate: I. Microbial degradation of organophosphorus compounds. *Geochim. Cosmochim. Acta* **61,** 4411–4422.

Bocherens H., Koch P. L., Mariotti A., Geraads D., and Jaeger J. J. (1996) Isotopic biogeochemistry (^{13}C, ^{18}O) of mammalian enamel from African Pleistocene hominid sites. *Palaios* **11,** 306–318.

Brunet M. and MPFT (2000) Chad: Discovery of a vertebrate fauna close to the Mio-Pliocene boundary. *J. Vert. Pal.* **20,** 205–209.

Brunet M., Beauvilain A., Coppens Y., Heintz E., Moutaye A. H. E., and Pilbeam D. (1995) The first australopithecine 2500 kilometers west of the Rift Valley (Chad). *Nature* **378,** 273–275.

Brunet M., Beauvilain A., Geraads D., Guy F., Kasser M., Mackaye H. T., MacLatchy L., Mouchelin G., Sudre J., and Vignaud P. (1997) Tchad: Un nouveau site à hominidés pliocène. *C. R. Acad. Sci. Paris* **324,** 341–345.

Brunet M., Beauvilain A., Geraads D., Guy F., Kasser M., Mackaye H. T., MacLatchy L. M., Mouchelin G., Sudre J., and Vignaud P.

(1998) Tchad: Découverte d'une faune de mammifères du Pliocène inférieur. *C. R. Acad. Sci. Paris* **326,** 153–158.

Bryant J. D. and Froelich P. N. (1995) A model of oxygen isotope fractionation in body water of large mammals. *Geochim. Cosmochim. Acta* **59,** 4523–4537.

Bryant J. D., Luz B., and Froelich P. N. (1994) Oxygen isotopic composition of fossil horse tooth phosphate as a record of continental paleoclimate. *Palaeogeogr. Palaeoclimatol. Palaeoecol.* **107,** 303–313.

Bryant J. D., Koch P. L., Froelich P. N., Showers W. J., and Genna B. J. (1996) Oxygen isotope partitioning between phosphate and carbonate in mammalian apatite. *Geochim. Cosmochim. Acta* **60,** 5145–5148.

Bunton C. A., Llewellyn D. R., Vernon C. A., Welch V. A. (1961) The reactions of organic phosphates. Part IV. Oxygen exchange between water and orthophosphoric acid. *J. Chem. Soc.* 1636–1640.

Crowson R. A., Showers W. J., Wright E. K., and Hoering T. C. (1991) A method for preparation of phosphate samples for oxygen isotope analysis. *Anal. Chem.* **63,** 2397–2400.

Driessens F. C. M. and Verbeeck R. M. H. (1990) *Biominerals*. CRC Press, Boca Raton, FL.

Fisher D. L. and Fox D. C. (1998) Oxygen isotopes in mammoth teeth: Sample design, mineralization patterns, and enamel-dentine comparisons. *J. Vert. Pal.* **18,** 41A–42A.

Fricke H. C. and O'Neil J. R. (1996) Inter- and intra-tooth variation in the oxygen isotope composition of mammalian tooth enamel phosphate: Implications for palaeoclimatological and palaeobiological research. *Palaeogeogr. Palaeoclimatol. Palaeoecol.* **126,** 91–99.

Fricke H. C., Clyde W. C., O'Neil J. R., and Gingerich P. D. (1998) Evidence for rapid climate change in north America during the latest Paleocene thermal maximum: Oxygen isotope compositions of biogenic phosphate from the Bighorn Basin (Wyoming). *Earth Planet. Sci. Lett.* **160,** 193–208.

Gadbury C., Todd L., Jahren A. H., and Amundson R. (2000) Spatial and temporal variations in the isotopic composition of bison tooth-enamel from the Early Holocene Hudson-Meng Bone Bed, Nebraska. *Palaeogeogr. Palaeoclimatol. Palaeoecol.* **157,** 79–93.

Geraads D., Brunet M., Mackaye H. T., and Vignaud P. (2001) Pliocene bovidae from the Koro Toro Australopithecine sites, Chad. *J. Vert. Pal.* **21 (*2*),** 335–346.

Gregory R. T. and Criss R. E. (1986) Isotopic exchange in open and closed systems. *Rev. Mineral.* **16,** 91–127.

Iacumin P., Bocherens H., Mariotti A., and Longinelli A. (1996) Oxygen isotope analyses of co-existing carbonate and phosphate in biogenic apatite: A way to monitor diagenetic alteration of bone phosphate? *Earth Planet. Sci. Lett.* **142,** 1–6.

IAEA/WMO (2001) Global Network of Isotopes in Precipitation. The GNIP Database. Accessible at http://isohis.iaea.org.

Ivany L. C., Patterson W. P., and Lohmann K. C. (2000) Cooler winters as a possible cause of mass extinctions at the Eocene/Oligocene boundary. *Nature* **407,** 887–890.

Jahnke R. A. (1984) The synthesis and solubility of carbonate fluorapatite. *Am. J. Sci.* **284,** 58–78.

Koch P. L., Fisher T. C., and Dettman D. L. (1989) Oxygen isotope variation in the tusk of extinct proboscideans: A measure of season of death and seasonality. *Geology* **17,** 515–519.

Koch P. L., Tuross N., and Fogel M. L. (1997) The effects of sample treatment and diagenesis on the isotopic integrity of carbonate in biogenic hydroxyapatite. *J. Arch. Sci.* **24,** 417–429.

Kohn M. J. (1996) Predicting animal $\delta^{18}O$: Accounting for diet and physiological adaptation. *Geochim. Cosmochim. Acta* **60,** 4811–4829.

Kohn M. J., Schoeninger M. J., and Barker W. W. (1999) Altered states: Effect of diagenesis on fossil tooth chemistry. *Geochim. Cosmochim. Acta* **63,** 2737–2747.

Kohn M. J., Schoeninger M. J., and Valley J. W. (1998) Variability in oxygen compositions of herbivore teeth: Reflections of seasonality or developmental physiology? *Chem. Geol. (Isot. Geosci. Sect.)* **152,** 97–112.

Kolodny Y. Luz B. (1991) Oxygen isotopes in phosphate of fossil fish—Devonian to recent. In *Stable Isotope Geochemistry: A Tribute to Samuel Epstein,* Spec. Publ. 3 (eds. Taylor, H. P. Jr., O'Neil, J. R. Kaplan, I. S.), pp. 105–119. The Geochemical Society.

Kolodny Y., Luz B., Sander M., and Clemens W. A. (1996) Dinosaur bones: Fossils or pseudomorphs? The pitfalls of physiology reconstruction from apatitic fossils. *Palaeogeogr. Palaeoclimatol. Palaeoecol.* **126,** 161–171.

Lécuyer C., Grandjean P., O'Neil J. R., Capetta H., and Martineau F. (1993) Thermal excursion in the ocean at the cretaceous-Tertiary boundary (northern Morocco): The $\delta^{18}O$ record of phosphatic fish debris. *Palaeogeogr. Palaeoclimatol. Palaeoecol.* **105,** 235–243.

Lécuyer C., Grandjean P., Barrat J.-A., Nolvak J., Emig C., Paris F., and Robardet M. (1998) $\delta^{18}O$ and REE contents of phosphatic brachiopods: A comparison between modern and lower Paleozoic populations. *Geochim. Cosmochim. Acta* **62,** 2429–2436.

Lécuyer C., Grandjean P., and Sheppard M. F. (1999) Oxygen isotope exchange between dissolved phosphate and water at temperatures ≤135°C: Inorganic versus biological fractionations. *Geochim. Cosmochim. Acta* **63,** 855–862.

Lee-Thorp J. A. and van der Merwe N. J.. (1987) Carbon isotope analysis of fossil bone apatite. *S. Afr. J. Sci.* **83,** 712–715.

LeGeros R. Z. and LeGeros J. P. (1984) Phosphate minerals in human tissues. In *Phosphate Minerals* (eds. J. O. Nriagu and P. B. Moore), pp. 352–385. Springer-Verlag, Berlin, Germany.

Longinelli A. (1984) Oxygen isotopes in mammal bone phosphate: A new tool for paleohydrological and paleohydrological research? *Geochim. Cosmochim. Acta* **48,** 385–390.

Luz B., Kolodny Y., and Horowitz M. (1984) Fractionation of oxygen isotopes between mammalian bone-phosphate and environmental drinking water. *Geochim. Cosmochim. Acta* **48,** 1689–1693.

Michel V., Ildefonse P., and Morin G. (1995) Chemical and structural changes in *Cervus elaphus* tooth enamels during fossilization (Lazaret cave): A combined IR and XRD Rietveld analysis. *Appl. Geochem.* **10,** 145–159.

Newesely H. (1989) Fossil bone apatite. *Appl. Geochem.* **4,** 233–245.

O'Neil J. R., Roe L. J., Reinhard E., and Blake R. E. (1994) A rapid and precise method of oxygen isotope analysis of biogenic phosphate. *Israel J. Earth Sci.* **43,** 203–212.

Passey B. H. and Cerling T. E. (2002) Tooth enamel mineralization in ungulates: Implications for recovering a primary isotopic time-series. *Geochim. Cosmochim. Acta* **66,** 3225–3234.

Person A., Bocherens H., Saliège J.-F., Paris F., Zeitoun V., and Gerard M. (1995) Early diagenetic evolution of bone phosphate: An X-ray diffractometry analysis. *J. Arch. Sci.* **22,** 211–221.

Posner A. (1987) Bone mineral and the mineralisation process. In *Bone and Mineral Research* (ed. W. A. Peck), pp. 65–116. Elsevier, New York.

Rink W. J. and Schwarcz H. P. (1995) Test for diagenesis in tooth enamel: ESR dating signals and carbonate content. *J. Arch. Sci.* **22,** 251–255.

Sen S. (1998) The age of the Molayan mammal locality, Afghanistan. *Geobios* **31,** 385–391.

Sen S. (2001) Rodents and insectivores from the Upper Miocene of Molayan, Afghanistan. *Paleontology* **44,** 913–932.

Shahack-Gross R., Tchernov E., and Luz B. (1999) Oxygen isotopic composition of mammalian skeletal phosphate from the Natufian period, Hayonim cave, Israël: Diagenesis and paleoclimate. *Geoarcheology* **14,** 1–13.

Sharp Z. D., Atudorei V., and Furrer H. (2000) The effect of diagenesis on oxygen isotope ratios of biogenic phosphates. *Am. J. Sci.* **300,** 222–237.

Shemesh A. (1990) Crystallinity and diagenesis of sedimentary apatites. *Geochim. Cosmochim. Acta* **54,** 2433–2438.

Shemesh A., Kolodny Y., and Luz B. (1988) Isotope geochemistry of oxygen and carbon in phosphate and carbonate of phosphorite francolite. *Geochim. Cosmochim. Acta* **52,** 2565–2572.

Soudry D. and Nathan Y. (2000) Microbial infestation: A pathway of fluorine enrichment in bone apatite fragments (Negev phosphorites, Israel). *Sediment. Geol.* **132,** 171–176.

Trautz O. R. (1967) Crystalline organization of dental mineral. In *Structural and Chemical Organization of Teeth* (ed. A. E. D. Miles), pp. 165–200. Academic Press, San Diego, CA.

Tuross N., Behrensmeyer A. K., Eanes E. D., Fisher L. W., and Hare P. E. (1989) Molecular preservation and crystallographic alterations in a weathering sequence of wildebeest bones. *Appl. Geochem.* **4,** 261–270.

Zazzo A (2001) Validation méthodologique de l'utilisation des compositions isotopiques (^{13}C, ^{18}O) des bioapatites fossiles pour la reconstitution des paléoenvironnements continentaux. Ph.D. dissertation, Univ. Pierre et Marie Curie, Paris.

Zazzo A., Bocherens H., Brunet M., Beauvilain A., Billiou D., Mackaye H. T., Vignaud P., and Mariotti A. (2000) Herbivore paleodiet and paleoenvironmental changes in Chad during the Pliocene using stable isotope ratios of tooth enamel carbonate. *Paleobiology* **26,** 294–309.

Zazzo A., Mariotti A., Lécuyer C., and Heintz E. (2002) Intra-tooth isotopic variations in Late Miocene bovid enamel from Afghanistan: Paleobiological, taphonomical, and climatical implications. *Palaeogeogr. Palaeoclimatol. Palaeoecol.* **186,** 145–161.

Zazzo A., Lécuyer C., Mariotti A. (2004) Experimentally-controlled carbon and oxygen isotope exchange between bioapatites and water under inorganic and microbially-mediated conditions. *Geochim. Cosmochim. Acta* **68,** 1–12.